Flexural behavior of precast concrete sandwich wall panels with basalt FRP and steel reinforcement

Douglas Tomlinson and Amir Fam

- A single-story precast concrete insulated sandwich wall panel design was tested in flexure using different shear-connector and flexural-reinforcement material types, namely steel and basalt-fiber-reinforced polymer (BFRP).
- BFRP connectors have the advantage of lower thermal bridging than conventional metallic connectors.
- The wall design performed adequately as a non-load-bearing wall based on building-code requirements for maximum wind pressure.

Space heating and cooling represent almost 60% of the energy consumption of commercial and residential structures in Canada. This is largely affected by the thermal resistance of the building envelope.[1] With regard to walls, designs with high thermal resistance (*R*-value) and thermal mass reduce required heating and cooling loads on a building relative to frame walls.[2,3] Prefabricated elements are advantageous in practice because they can be constructed quickly in a controlled environment by a single manufacturer, then shipped to the site to quickly close the building envelope.[4] Precast concrete insulated wall panels are prefabricated elements that combine structural and thermal efficiency. These panels are typically composed of a 25 to 100 mm (1 to 4 in.) thick rigid layer of foam insulation surrounded by two wythes of reinforced concrete.[5] Wythe thickness depends on expected loads, fire, and cover requirements and generally ranges from 50 to 150 mm (2 to 6 in.).[6]

The structural behavior of sandwich panels heavily depends on the shear force transferred between wythes through elements known as connectors. Connectors are commonly arranged as discrete ties, trusses,[7,8] mesh grids,[9] or solid concrete regions.[10] They have been composed of various materials, including steel, fiber-reinforced polymers (FRPs), and plastics.[5] Panels with complete shear transfer are termed fully composite, panels with no transfer

are termed noncomposite, and panels with some shear transfer between the two are termed partially composite[6] Partial and noncomposite walls are also characterized through broken-line strain profiles (that is, two neutral axes) that create strain discontinuity between the wythes. This discontinuity accumulates over the panel length as relative slip between the wythes (shear deformation), which is greatest at the panel ends.[11]

There are advantages to both fully composite and noncomposite walls. Fully composite walls are stronger and stiffer but are more susceptible to thermal bowing, which is of particular concern in long walls.[5] Fully composite walls are also more susceptible to reduced *R*-values because of thermal bridging.[12] Fully composite and noncomposite panels can be readily analyzed using reinforced concrete sectional analysis, but there is uncertainty in evaluating partial composite panels because their behavior is much more complex and typically relies on test results and designer experience.[5] If the level of composite action is quantified, it allows designers to more accurately design a wall system.

Composite action has been evaluated using numerous methods, including strength, deflection,[13] stresses,[8] effective moment of inertia,[14] and curvature.[9] Previous test programs for direct shear and flexure have seen high or full degrees of composite action from heavy steel trusses[8] or solid concrete regions[14] as shear connectors. Less composite action has been observed in sections with discrete steel, FRP, or plastic ties.[15] High degrees of composite action with reduced thermal bridging have also been achieved using glass-fiber-reinforced polymer (GFRP) trusses[7] and carbon-fiber-reinforced polymer (CFRP) grids.[9]

Panel insulation is typically composed of expanded polystyrene or extruded polystyrene because these foams can withstand the pressure and temperature of concrete casting, provide the desired *R*-values, and act as stay-in-place formwork. The foam layer has been found to contribute significantly to composite action,[13,16] with expanded polystyrene giving higher values in addition to often being less costly.[2]

Basalt-fiber-reinforced polymer (BFRP) has recently been used in concrete structures as flexural reinforcement and shear connectors.[17–19] Relative to GFRP, BFRP is promising because it is stronger and stiffer while having similar durability and thermal conductivity.[20] BFRP is less costly than CFRP[21] and is easier to manufacture than GFRP and CFRP.[17]

This paper investigates the composite action of a nonprestressed concrete insulated wall panel using four-point bending tests. The impact of varying shear-connector and longitudinal-reinforcement material between steel and BFRP is studied, and the performance of full walls with that of the structural wythe alone is compared. The results focus on the flexural-test results compared with theoretical values to quantify the level of composite action. Digital image correlation is also used to aid the understanding of wythe slip.

Experimental program

Panel design

A single-story, two-wythe, nonprestressed sandwich panel design (**Fig. 1**) forms the basis for this study. Each panel is 2700 mm (106.3 in.) long, 1200 mm (47 in.) wide, and 270 mm (11 in.) thick. The facade (exterior) wythe has a rectangular cross section with a thickness of 60 mm (2.4 in.); the structural (interior) wythe has a double-tee cross section with a 60 mm thick flange and 150 mm (5.9 in.) deep webs spaced center to center at 600 mm (24 in.). The bulb-shaped webs are between 50 and 70 mm (2 and 3 in.) and extend into the insulation layer. The bulb accommodates longitudinal reinforcement. The webs serve to increase the structural wythe's flexural resistance while reducing the unsupported shear-connector length through the insulation. This increases composite action without sacrificing much thermal insulation. The insulation for all panels in this study was made of expanded polystyrene.

Panels were reinforced for flexure with steel or BFRP bars. In steel-reinforced sections, the facade wythe and flange of the structural wythe were each reinforced at mid-thickness with a welded reinforcement grid of D5 (0.25 in. diameter) bars spaced at 200 mm (8 in.) transversely and longitudinally. The flange of the structural wythe was also reinforced at mid-thickness with an additional longitudinal D8 (0.32 in. diameter) bar bundled to the mesh at each flange-web junction. A single D8 bar was also placed in each web 120 mm (5 in.) from the face of the structural wythe. BFRP-reinforced panels had the same arrangement, but the D5 mesh was replaced with nominal 6 mm (0.24 in.) diameter BFRP bars, while the D8 bars were replaced with nominal 8 mm (0.31 in.) diameter BFRP bars. The 100 mm (4 in.) section at each end of the structural wythe consists of solid reinforced concrete headers, which are intended to accommodate bolted connection hardware and serve as lintel beams for axial load bearing in practice. The headers were transversely reinforced with four 10M (no. 3) steel bars or 10 mm (0.39 in.) nominal diameter BFRP bars.

The panels had discrete shear connectors (**Fig. 2**) spaced longitudinally at 600 mm (24 in.). Connectors were inserted through the facade wythe into the web of the structural wythe. The steel connectors consisted of two L-shaped D5 (0.25 in. diameter) bars, one inserted normal to the facade and the other placed at a 45-degree angle. The connectors were laid out such that they would be put into tension if the panel were subjected to external pressure. BFRP connector pairs were cut into a U shape from a 6 mm (0.24 in.) nominal diameter, 600 × 600 mm square spiral tie and inserted into the panel at the desired angles, again one normal to the facade and one at a 45-degree angle.

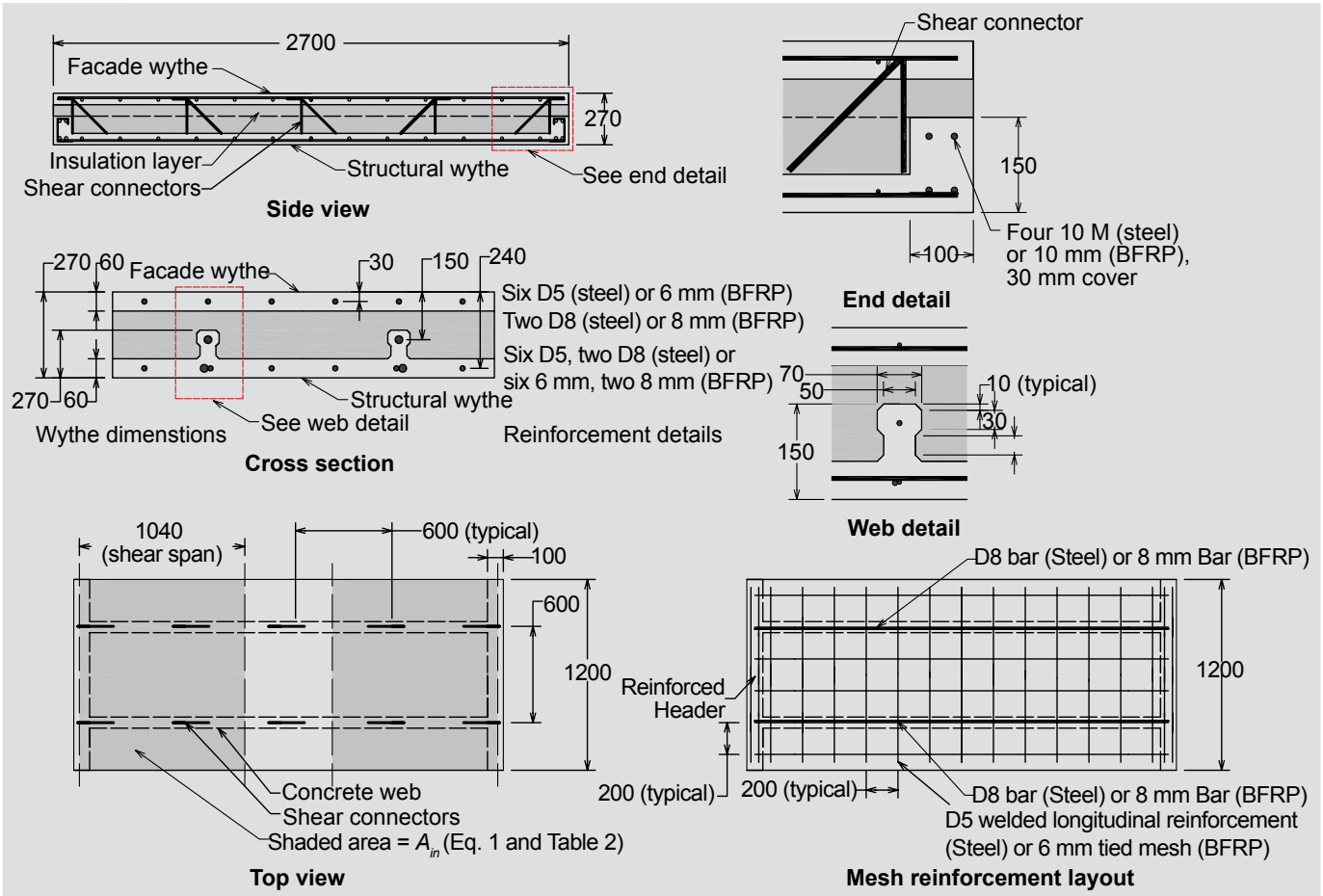

Figure 1. General panel design. Note: A_{in} = insulation foam area subject to shear; BFRP = basalt-fiber-reinforced polymer. All dimensions are in millimeters. 1 mm = 0.0394 in.

The *R*-value of the panels, calculated using the revised zone method from Lee and Pessiki,[10] is 2.86 m^2 K/W (19.8 h × ft^2 °F/BTU) for panels with steel connectors and 3.10 m^2K/W (21.5 h × ft^2°F/BTU) for panels with BFRP connectors. Both values meet the ASHRAE 90.1 zone 7[22] requirements for mass walls.

Material properties

All of the panels used the same mixture proportions but were cast on four separate dates. The concrete used in the panels was self-consolidating, with a design flow of 650 and 700 mm (26 and 28 in.), a maximum aggregate size of 6 mm (0.24 in.), a one-day stripping strength of 30 MPa (4.3 ksi), and a design 28-day compressive strength of 60 MPa (8.7 ksi). Test-date cylinder tests gave strengths from 58 to 70 MPa (8.3 and 10 ksi).

Steel used for the shear connectors and flexural reinforcement was made from deformed bars with a yield strength of 485 MPa (70 ksi), ultimate strength of 650 MPa (94 ksi), and elastic modulus of 196 GPa (28,400 ksi), based on standard tension tests (**Fig. 3**). The D5 (0.25 in. diameter) and D8 (0.32 in. diameter) bars have cross-sectional areas of 31 and 51 mm^2 (0.048 and 0.079 $in.^2$), respectively.

The BFRP bars have a specified tensile elastic modulus of 70 GPa (10,000 ksi) and guaranteed ultimate tensile strength of 1100 MPa (160 ksi), based on manufacturer data. Two nominal bar diameters of 6 and 8 mm (0.24 and 0.31 in.) were used, and their cross-sectional areas, determined through immersion tests, were 28 and 59 mm^2 (0.043 and 0.091 $in.^2$), respectively. Tensile test results of the 6 mm (0.24 in.) diameter bars gave strengths of 1132 and 1185 MPa (164.2 to 171.8 ksi) and elastic moduli between 65 and 73 GPa (9400 and 10,400 ksi) (Fig. 3).

Expanded polystyrene foam with a density of 27 kg/m^3 (1.7 lb/ft^3) was used as insulation because it is available precut and in greater thicknesses than extruded polystyrene, eliminating the time required to cut and adhere layers of extruded polystyrene foam. The insulation was also infused with graphite to improve its *R*-value. Material tests (Fig. 3) showed that the insulation has a yield strength of 122 kPa (17.7 ksi) at 1.67% strain, an elastic modulus of 9.2 MPa (1.3 ksi), and a shear modulus G_{in} (Eq. [1]) of 5.7 MPa (0.83 ksi).

Test specimens and parameters

To investigate this panel design and compare the two reinforcement and shear-connector materials, seven flexural tests

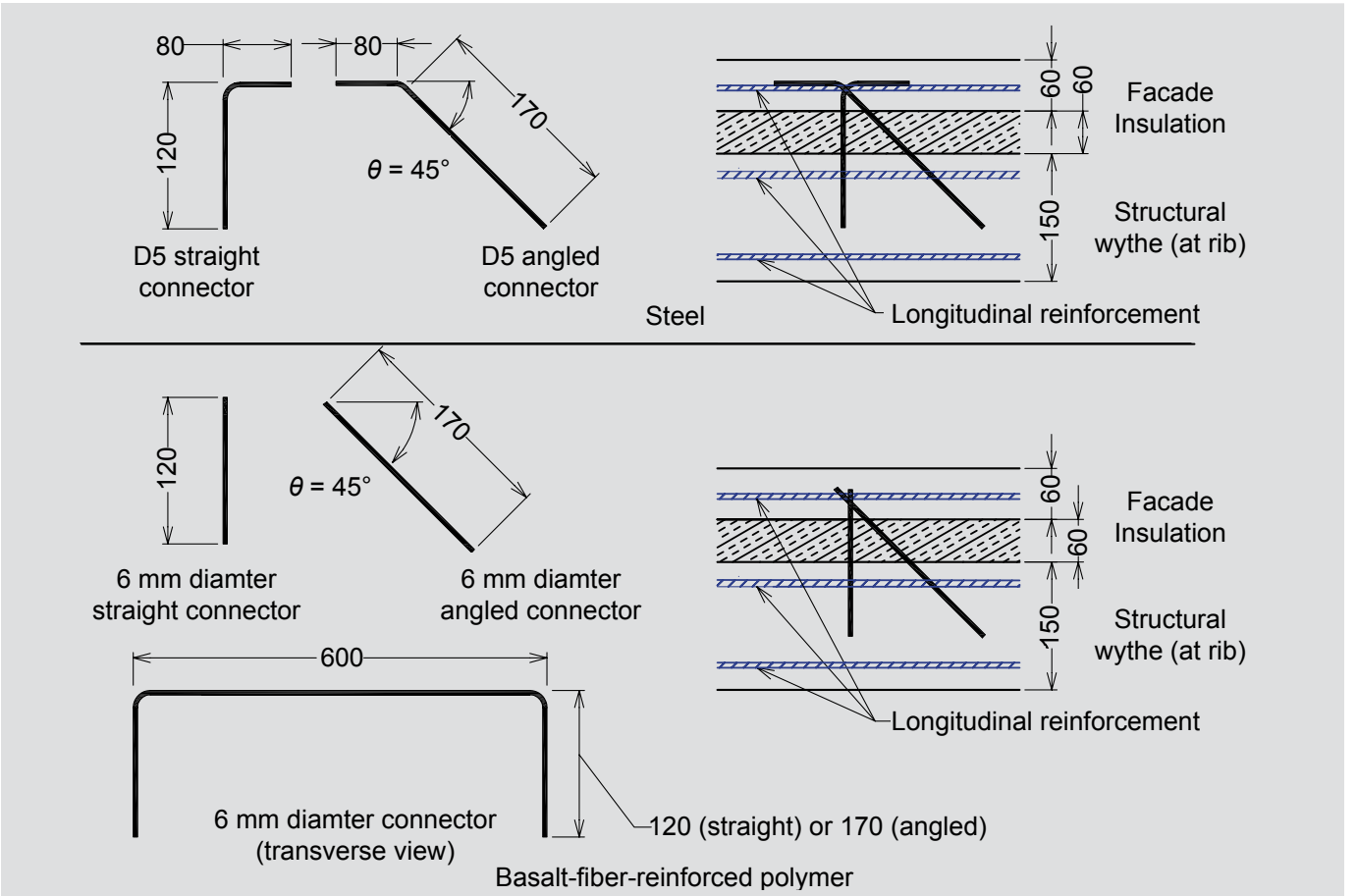

Figure 2. Dimensions and layout of shear connector pair. Note: All dimensions are in millimeters. 1 mm = 0.0394 in.

were performed (**Table 1**). The control test (specimen SPF) was a full panel reinforced with steel longitudinal bars and steel shear connectors with loads applied to the facade wythe to simulate wind pressure. Specimen SSF was identical to specimen SPF except that bending load was applied in the opposite direction (that is, loading on the structural wythe) to simulate wind suction.

To investigate the facade layer's contribution to partial composite action, specimens SPS and SSS, which consist of only the structural wythes, were tested with the ribs of specimen SPS on the compression side for the wind-pressure case, and the ribs of specimen SSS on the tension side for the wind-suction case. Specimen HPF has the same flexural design as specimen SPF (that is, flexural steel reinforcement) but has BFRP shear connectors to capitalize on the reduced thermal bridging through the shear connectors and to investigate the impact of the lower stiffness of BFRP connectors, compared with steel connectors, on panel response.

To evaluate the performance of an all-FRP-reinforced system (for flexure and connectors), which may allow for thinner wythes in the future due to reduced cover requirements, two fully BFRP-reinforced walls were tested, with specimen BPF being the full panel and specimen BPS being the structural wythe only. Both panels were tested in the pressure configuration.

The reinforcement ratios of the steel- and BFRP-reinforced panels were intended to be equal but varied by as much as 7%. Both materials were provided in the standard reinforcement configuration (Fig. 1) using the available bar sizes for each material type. Equal reinforcement ratios were considered rather than designing for equal stiffness. This allowed for better assessment of the panel-fabrication process, based on fully composite sectional properties and considering the greater strength of BFRP compared with steel. The BFRP-reinforced walls had similar strength to their steel-reinforced counterparts (varying from 7% [fully composite] to 13% stronger [noncomposite]). All walls satisfied the minimum longitudinal reinforcement ratio of 0.15% and transverse reinforcement ratio of 0.2% of the gross concrete cross-sectional area A_g given by CSA A23.3-04[23] and ACI 318-14.[24]

The effective shear-connection stiffness G_c[11] was evaluated using Eq. (1):

$$G_c = nE_{sc}A_{sc}(\sin\theta) + G_{in}A_{in} \quad (1)$$

where

n = number of shear connectors

E_{sc} = shear-connector modulus of elasticity

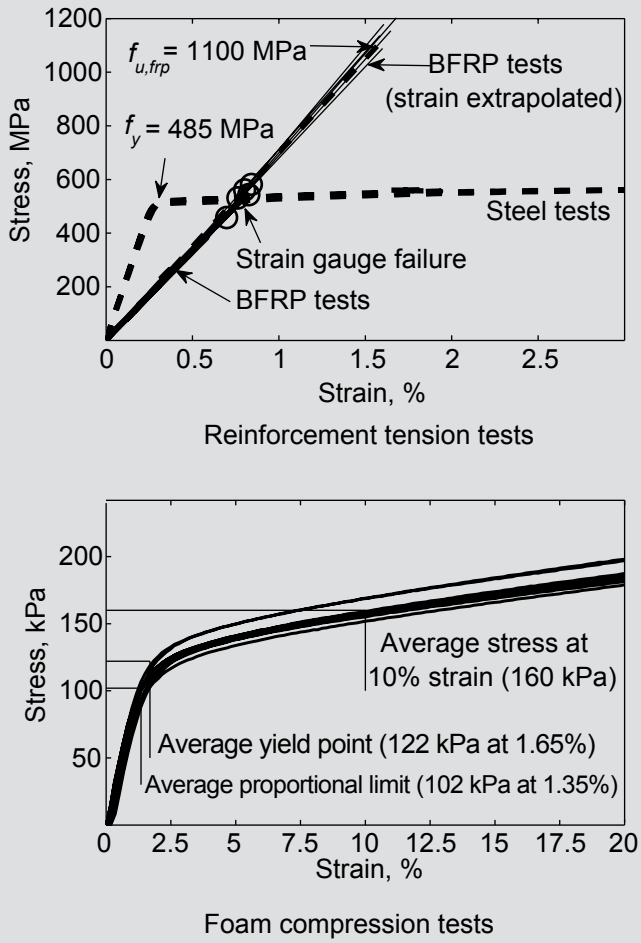

Figure 3. Material properties. Note: BFRP = basalt-fiber-reinforced polymer. 1 kPa = 0.145 psi; 1 MPa = 0.145 ksi.

A_{sc} = shear-connector cross-sectional area

θ = connector insertion angle

G_{in} = shear modulus of the insulation foam

A_{in} = area of foam subjected to shear at the facade wythe, which is the minimum contact area (Fig. 1)

At low slip values, it has been found that perpendicular shear connectors have a negligible impact on shear stiffness and their contribution from dowel action was ignored.[19] **Table 2** presents the inputs and evaluation of G_c for the tested panels.

Fabrication process

The panels were fabricated at a precast concrete facility (Fig. 4). The expanded polystyrene foam sections were cut using a computer numerical control machine. The reinforcement was then cut to size. The steel reinforcement was prewelded, while the BFRP reinforcement was tied with plastic zip ties. Shear connectors were inserted after setting the longitudinal bar in the web and placing the facade mesh. Steel shear connectors were made by cutting D5 (0.25 in.) bars, then bending them to 90-degree or 135-degree angles (Fig. 2). BFRP connectors were cut from a prefabricated spiral. The connectors were tied to both the facade mesh and the web reinforcement for continuity. The panel was flipped, and the structural wythe flange mesh was added. The foam and reinforcement were then inserted into a steel form and poured vertically. To prevent floating of the foam during casting, the top of the panel was restrained by steel sections bolted to the formwork. Most panels were cast with a brick facade with negligible structural contribution that added 8 mm (0.3 in.) to the facade wythe thickness. Panels were stripped after one day and stored flat (facade side down), spending one week indoors, then an additional three- to six-month period outdoors before being shipped facade side down via flatbed truck to the testing facility. During storage, the panels were exposed to temperature ranges of −29 to +27°C (−20 to +81°F) in addition to rain and snow.

Test setup and instrumentation

Each panel was tested in four-point bending to failure under stroke control at 2 mm/min (0.08 in/min) using a 223 kN (50.1 kip) hydraulic actuator. The panels had a span of 2630 mm (104 in.), a constant moment zone of 550 mm (22 in.), and shear spans of 1040 mm (41 in.) (**Fig. 5**). At each end, the panel was plastered to a 102 mm (4.02 in.) wide and 12.7 mm (0.5 in.) thick steel plate bearing against a 32 mm (1.3 in.) diameter round bar to create roller connections. At the central loading points, two 102 × 102 × 12.7 mm hollow structural sections were used to distribute load across the width of the panel to ensure one-way behavior.

Load was measured with the actuator's load cell. Deflections at midspan, the ends of the constant moment zone, and midway through the shear span were recorded with 100 mm (4 in.) linear potentiometers (Fig. 5). Two additional 100 mm linear potentiometers were attached to the panel ends to measure relative slip between the wythes. Midspan longitudinal reinforcement strains were measured with 5 mm (0.2 in.) 120 Ω strain gauges mounted on each bar layer (Fig. 5). Strains at the top concrete surface were measured with two 50 mm (2 in.) 120 Ω strain gauges placed 300 mm (12 in.) from each edge of the panel. Strains were also found with 100 mm displacement-type pi gauges. The pi gauges were also used to develop wythe moment-curvature relationships. They were placed 10 mm (0.4 in.) from the top and bottom surface of the panel and 10 mm from the edges of each wythe. The 10 mm offset was included in curvature calculations. To complement the slip linear potentiometer readings, digital image correlation was used on one end of the panel. A camera with a 5184 × 3456 pixel image size was used to photograph the 400 mm (16 in.) end of the panel at 15-second intervals during each test. Digital image correlation was then performed using a software

Inserting basalt-fiber-reinforced polymer shear connector

Foam and facade reinforcement

Structural wythe chair to reduce stress on foam during casting

Final product with nonstructural architectural facade

Foam and reinforcement before closing of form

Figure 4. Fabrication of test panels.

program.[25] Digital image correlation tracks the movement of a superimposed mesh of 64 × 64 pixel texture patches over the course of a test and reports a matrix of horizontal and vertical movements for each patch. This has previously been used to evaluate panel end slip[19] and has been extended to present wythe rotation in this work (**Fig. 6**).

Table 1. Test matrix for flexure tests

Specimen	Longitudinal reinforcement material	Shear connector material	Loading condition	Panel type	Wall reinforcement, % of A_g	Reinforcement stiffness EA, $\times 10^6$ N	Shear connection stiffness G_c, $\times 10^6$ N	Concrete strength, MPa
SPF	Steel	Steel	Pressure	Full	0.38	115.3	48.5	57.7
SSF	Steel	Steel	Suction	Full	0.38	115.3	48.5	57.5
SPS	Steel	None	Pressure	Structural	0.48	77.6	n/a	63.0
SSS	Steel	None	Suction	Structural	0.48	77.6	n/a	61.6
HPF	Steel	BFRP	Pressure	Full	0.38	115.3	25.2	70.4
BPF	BFRP	BFRP	Pressure	Full	0.37	40.0	25.2	60.9
BPS	BFRP	None	Pressure	Structural	0.49	28.3	n/a	69.3

Note: A = gross reinforcement cross-sectional area; A_g = gross concrete cross-sectional area; BFRP = basalt-fiber-reinforced polymer; BPF = full panel BFRP-reinforced wall; BPS = structural wythe BFRP-reinforced wall; HPF = same flexural design as SPF but has BFRP shear connectors; E = reinforcment elastic modulus; n/a = not applicable; SPF = control full-panel reinforced with steel longitudinal bars and steel shear connectors with the load applied to the facade wythe; SPS = structural wythe with the ribs on the compression side; SSF = identical to SPF except load applied on the structural wythe; SSS = structural wythe with the ribs on the tension side. 1 N = 0.225 lb; 1 MPa = 145 psi.

Results and discussion

The general response and failure mode of each panel were heavily reliant on the longitudinal reinforcement material. The test results (**Table 3**) include the self-weight of the panel and spreader beams as part of the reported loads because they accounted for 7% to 17% of the ultimate load. The maximum service live load *LL* for each panel was determined to be the lowest value given by three commonly used constraints. The first constraint is from strength, which unfactors the ultimate load *UL* using the *UL* equal to 1.25*DL* + 1.5*LL* load factors in the *National Building Code of Canada*,[26] assuming that the dead load *DL* is the self-weight and spreader-beam weight. The second constraint limits midspan deflection from live load to *L*/360, commonly used for architectural features, where *L* is the span length (this is stricter than the limit of *L*/150 for wall elements). The final constraint is strain, with three strain limits being examined: the point where concrete strain exceeds 0.001, accepted as where concrete becomes nonlinear; the FRP strain of 0.002, where the crack widths are expected to exceed acceptable values;[27] or when the steel strain exceeds 60% of yield. **Table 4** summarizes the service load values for each panel using these three conditions.

Ductility in sections that yielded was evaluated using the ductility index $\Delta u/\Delta y$ (where Δu is the midspan deflection at ultimate and Δy is the midspan deflection at yielding). Also, deformability Φ was evaluated using the J-factor (Eq. [2]):[28]

Table 2. Shear connector stiffness inputs

Specimen	Shear connector					Insulation			G_c, $\times 10^6$ N
	n	E_{sc}, MPa	A_{sc}, mm^2	θ, deg	Shear connector contribution, $\times 10^6$ N	A_{in}, m^2	G_{in}, MPa	Insulation contribution, $\times 10^6$ N	
SPF	8	196	31	45	34.4	2.47	5.7	14.1	48.5
SSF	8	196	31	45	34.4	2.47	5.7	14.1	48.5
HPF	8	70	28	45	11.1	2.47	5.7	14.1	25.2
BPF	8	70	28	45	11.1	2.47	5.7	14.1	25.2

Note: SPS, SSS, and BPS only consist of a structural wythe and have no shear connection stiffness. A_{in} = insulation foam area subject to shear; A_{sc} = shear connector cross-sectional area; FRP = basalt-fiber-reinforced polymer; BPF = full panel BFRP-reinforced wall; BPS = structural wythe BFRP-reinforced wall; E_{sc} = shear connector elastic modulus; G_c = effective shear-connection stiffness accounting for both connector and insulation contribution; G_{in} = shear modulus of insulation foam; HPF = same flexural design as SPF but has BFRP shear connectors; n = number of shear connectors; SPF = control full-panel reinforced with steel longitudinal bars and steel shear connectors with the load applied to the facade wythe; SPS = structural wythe with the ribs on the compression side; SSF = identical to SPF except load applied on the structural wythe; SSS = structural wythe with the ribs on the tension side; θ = shear connector insertion angle. 1 mm = 0.0394 in.; 1 m = 3.28 ft; 1 N = 0.225 lb; 1 MPa = 145 psi.

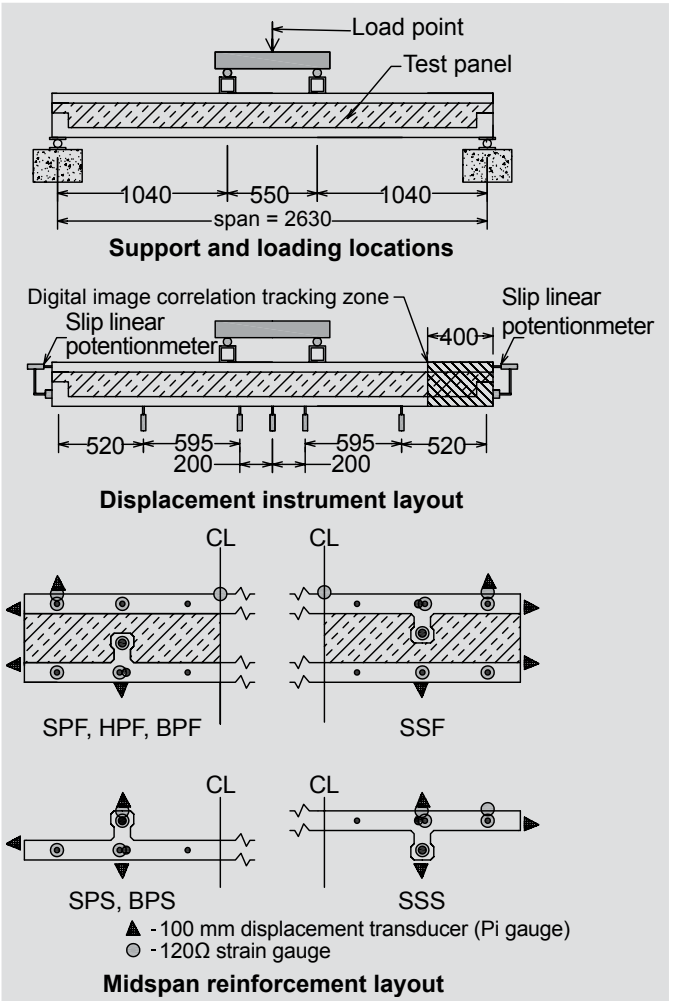

Figure 5. Test setup and instrumentation locations. Note: BFRP = basalt-fiber-reinforced polymer; BPF = full panel BFRP-reinforced wall; BPS = structural wythe BFRP-reinforced wall; DIC = digital image correlation; HPF = same flexural design as SPF but has BFRP shear connectors; SPF = control full-panel reinforced with steel longitudinal bars and steel shear connectors with the load applied to the facade wythe; SPS = structural wythe with the ribs on the compression side; SSF = identical to SPF except load applied on the structural wythe; SSS = structural wythe with the ribs on the tension side. All dimensions are in millimeters. 1 mm = 0.0394 in.

$$\Phi = \frac{\delta_u}{\delta_{NL}} \times \frac{M_u}{M_{NL}} \qquad (2)$$

where

δ_u = deflection at ultimate

δ_{NL} = deflection at the point of nonlinearity

M_u = ultimate moment

M_{NL} = moment at the point of nonlinearity

Although curvature is more commonly used than deflection to evaluate deformability, these panels have considerable shear deformations and curvature was unable

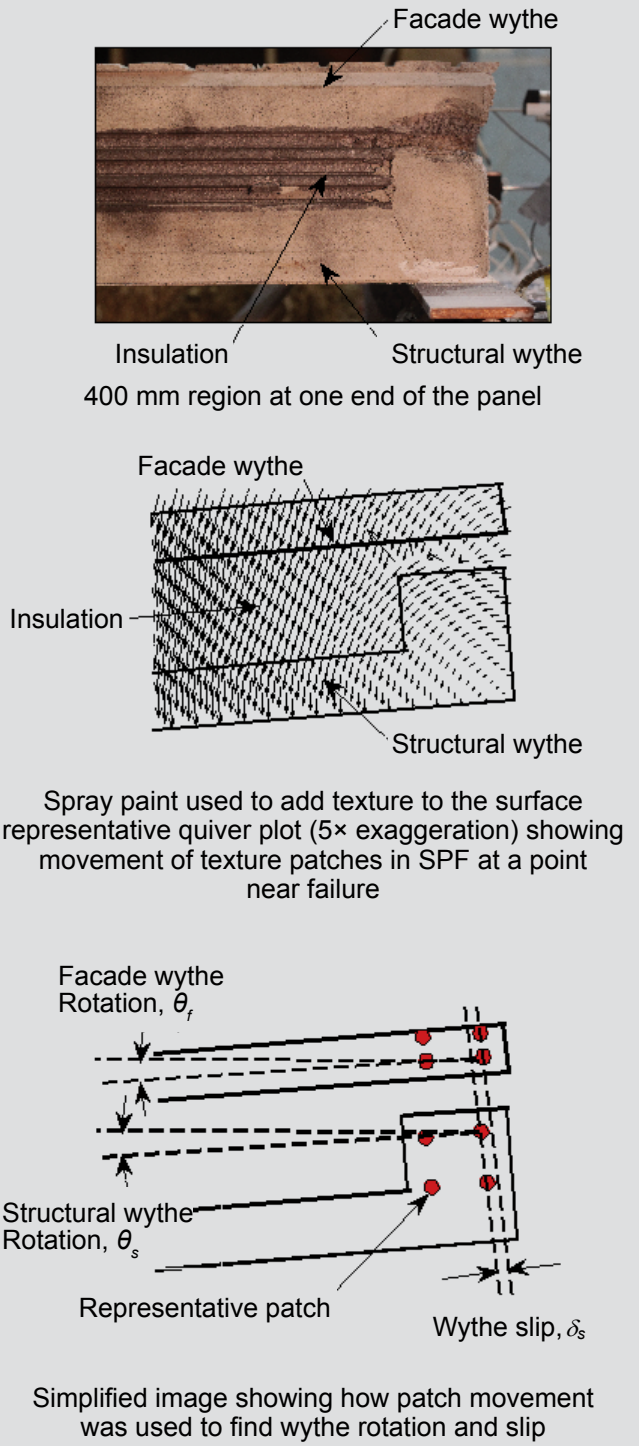

Figure 6. Use of digital image correlation in experimental program. Note: SPF = control full-panel reinforced with steel longitudinal bars and steel shear connectors with the load applied to the facade wythe. 1 mm = 0.0394 in.

to capture the true panel deformability. The point of nonlinearity was taken as the lowest of reinforcement yielding, concrete compression strain exceeding 0.001, and the point when the end slip exceeds the linear region established in prior push-through tests.[19] Deformability was also found using energy methods by taking the ratio of strain energy at ultimate to strain energy at the point of

Table 3. Key results from flexural tests

		Specimen						
		SPF	SSF	SPS	SSS	HPF	BPF	BPS
Key load points, kN	Ultimate	99.3	72.7	41.4	26.3	88.9	58.6	35.7
	Yielding	74.6	58.5	33.9	21.8	67.0	n/a	n/a
	Nonlinearity*	69.1	58.5	30.8	21.8	54.6	45.0	21.9
	Service	50.9	50.8	23.5	16.6	39.4	29.5	17.0
	Cracking	22.7	18.2	20.7	12.0	21.2	20.1	16.1
Total end slip, mm	Ultimate	7.08	1.87	n/a	n/a	12.18	16.43	n/a
	Yielding	1.87	1.11	n/a	n/a	4.27	n/a	n/a
	Nonlinearity*	1.66	1.11	n/a	n/a	3.08	3.47	n/a
	Service	0.84	0.67	n/a	n/a	1.74	1.14	n/a
Deflection, mm	Ultimate	45.1	33.7	36.9	42.9	54.9	64.2	67.5
	Yielding	14.1	11.2	16.4	16.9	17.5	n/a	n/a
	Nonlinearity*	12.4	11.2	14.2	16.9	12.6	18.3	25.0
	Service	7.6	8.7	7.8	8.0	7.8	6.6	8.3
Strain energy, kN-mm	Ultimate	3512	2079	1192	9.6	3819	2921	1671
	Yielding	650	365	392	270	731	n/a	n/a
	Nonlinearity*	551	365	316	270	452	555	333
	Service	243	306	119	95	206	117	96
Ductility		3.20	3.02	2.25	2.54	3.14	n/a	n/a
Deformability	J factor	5.22	3.73	3.49	3.06	7.08	4.59	4.41
	Energy	6.37	5.70	3.77	3.34	8.45	5.26	5.02
Failure mode		Longitudinal bar rupture	Longitudinal bar rupture	Longitudinal bar rupture	Longitudinal bar rupture	Longitudinal bar rupture	Shear connector failure/ compression	Shear compression

Note: BFRP = basalt-fiber-reinforced polymer; BPF = full panel BFRP-reinforced wall; BPS = structural wythe BFRP-reinforced wall; HPF = same flexural design as SPF but has BFRP shear connectors; n/a = not applicable; SPF = control full-panel reinforced with steel longitudinal bars and steel shear connectors with the load applied to the facade wythe; SPS = structural wythe with the ribs on the compression side; SSF = identical to SPF except load applied on the structural wythe; SSS = structural wythe with the ribs on the tension side; ε_c = concrete strain. 1 mm = 0.0394 in.; 1 kN = 0.225 kip.

* The point of nonlinearity was set to occur at the lowest of yielding, $\varepsilon_c > 0.001$, and end slip exceeding linear values found in previous push-through tests. This was used to determine deformability.

nonlinearity. Table 3 presents a summary of ductility and deformability factors.

Behavior of steel-reinforced panels

Fig. 7 shows the load-deflection plots of steel-reinforced panels, and **Fig. 8** shows photos of the panels taken during testing. The steel-reinforced panels had a high initial stiffness until cracking. Crack formation was audible and indicated by a decrease in stiffness. These decreases were most pronounced in specimen SPS because the cross section has a high percentage of concrete in tension. Yielding occurred at similar deflections in each panel but yield load increased with reinforcement percentage and shear-connection stiffness. Due to the multiple layers of reinforcement and the relatively high yield strength of the steel, the load continued to increase after initial yielding, though at reduced stiffness. Near ultimate, the second layer of steel also yielded. Ultimate occurred after an additional 17% to 33% increase in load beyond yielding. After ultimate was

Table 4. Maximum service load values from each method

Specimen	Maximum service load, kN				Service load governed by:
	Back-calculated from ultimate	Deflection (>L/360)	Concrete strain, (>1000 με)	Reinforcement strain*	
SPF	52.1	50.9†	68.2	51.9	Deflection
SSF	41.4†	62.2	63.7	53.1	Strength
SPS	24.7	24.1	30.8	23.8†	Reinforcement strain
SSS	19.0	16.6†	24.2	17.5	Deflection
HPF	47.6	40.0†	46.7	40.2	Deflection
BPF	38.1	34.6	40.2	22.3†	Reinforcement strain
BPS	25.2	17.3†	20.1	18.3	Deflection

Note: BFRP = basalt-fiber-reinforced polymer; BPF = full panel BFRP-reinforced wall; BPS = structural wythe BFRP-reinforced wall; f_y = steel yield stress; HPF = same flexural design as SPF but has BFRP shear connectors; L = span length; SPF = control full-panel reinforced with steel longitudinal bars and steel shear connectors with the load applied to the facade wythe; SPS = structural wythe with the ribs on the compression side; SSF = identical to SPF except load applied on the structural wythe; SSS = structural wythe with the ribs on the tension side. 1 kN = 0.225 kip.
*Steel-reinforced panel maximum service strain = $0.6f_y$ = 2475 με. BFRP-reinforced panel maximum service strain = 2000 με.
†Governing value for each panel.

reached, the load steadily decreased as the flexural reinforcement necked then ruptured (Fig. 8).

Rupture was expected as the reinforcement ratio is small, the concrete strength is relatively high, and the steel-welded longitudinal reinforcement is brittle relative to mild-steel reinforcement, which would allow for greater curvature to be developed and makes crushing more likely to occur. In general, Fig. 7 shows that partial composite behavior has a significant contribution to flexural strength, whether the panel simulates wind pressure (specimen SPF versus specimen SPS) or suction (specimen SSF versus specimen SSS). The ultimate load increased 2.49 times in pressure and 2.99 times in suction. Also, hybrid specimen HPF with flexural steel reinforcement and BFRP ties behaved somewhat similarly to all-steel specimen SPF but with slightly lower strength and stiffness. In this hybrid specimen, partial composite behavior increased the ultimate load 2.21 times.

For steel-reinforced full panels (specimens SPF, SSF, and HPF) (that is, panels with both wythes) the load–end slip relationships in **Fig. 9** showed similar shapes to the load-deflection plots. Specimens SPF and SSF showed nearly identical load-slip relationships until ultimate. Connector yielding was observed in specimen SPF and, although this was not the cause of failure, it prevented the full composite load from being reached. The side of the panel (longitudinal direction) where connectors yielded saw greater shear deformation after that point relative to the other side (Fig. 8). Connectors in specimen SSF did not reach material failure because slip did not exceed the point of connector buckling seen in prior push-through tests.[19] Specimen HPF had higher slip under the same loads as specimen SPF due to the lower stiffness of the BFRP connectors. The connectors closest to the support on one side (longitudinal direction) of specimen HPF failed around yielding of the longitudinal reinforcement and caused end slip to greatly increase on that side only. However, the load in specimen HPF continued to increase until flexural failure occurred.

In the full panels, the strain readings (**Fig. 10**) in the extreme compression fiber were well below crushing and indicate that the panels were severely underreinforced. Plane sections did not remain plane because there was discontinuity in the strain profile for the panels through the foam layer. In pressure cases, this led to compressive strains at the top of the web and tension at the bottom of the facade wythe. Panels with only the structural wythe, however, had strains nearing crushing at ultimate.

Behavior of BFRP-reinforced panels

Specimens BPF and BPS had lower postcracking stiffness than their steel-reinforced counterparts (Fig. 7). Cracking was clearly audible and caused larger decreases in load and longer recovery periods than for specimens SPF and SPS. The panel stiffness decreased further when the second series of cracks formed at a load of 31.2 kN (7.01 kip). From this point, specimen BPF remained essentially linear as cracking propagated until the load reached 52.7 kN (11.8 kip). At this point, the outermost shear connectors at one end of the panel failed, which decreased demand on the flexural reinforcement and increased end slip (Fig. 8 and 9). This also caused a change in the panel's deflected shape as the greatest deflection no longer occurred at midspan because shear deformation began to dominate on one

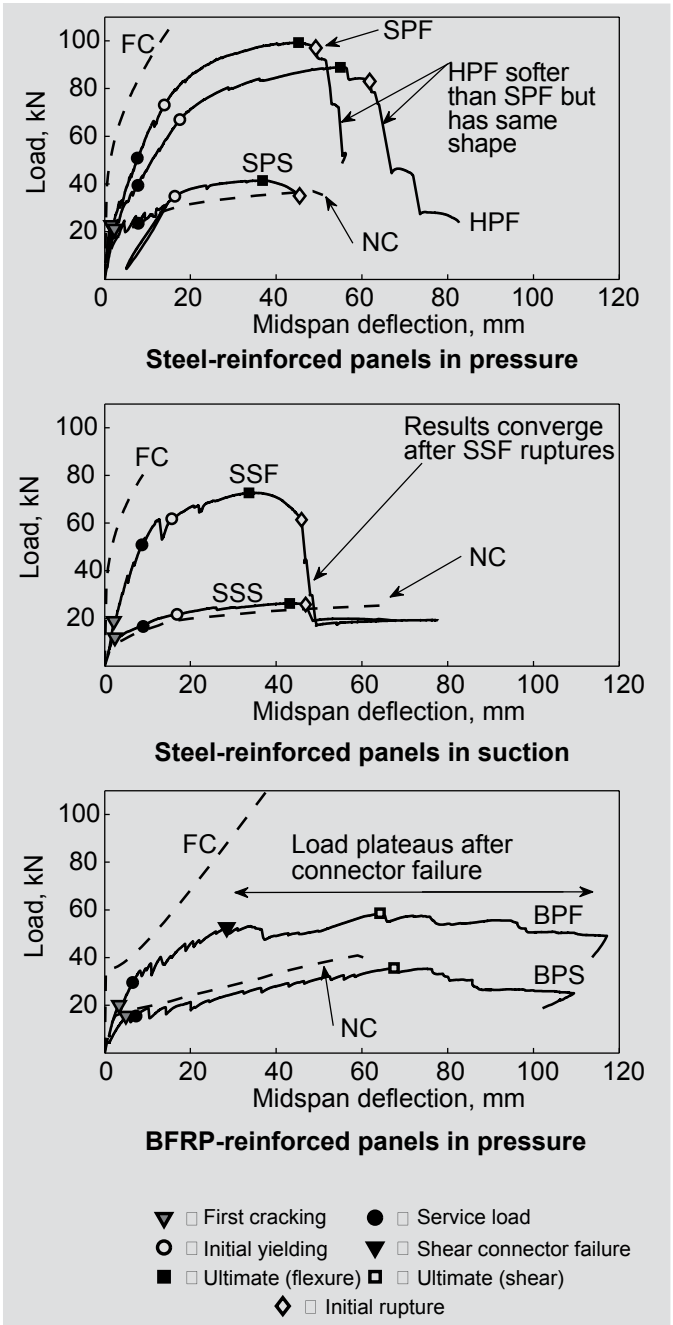

Figure 7. Load-midspan deflection relationships for each test. Theoretical curves for FC and NC walls are shown. Note: Values include self-weight. BFRP = basalt-fiber-reinforced polymer; BPF = full panel BFRP-reinforced wall; BPS = structural wythe BFRP-reinforced wall; FC = fully composite; HPF = same flexural design as SPF but has BFRP shear connectors; NC = noncomposite; SPF = control full-panel reinforced with steel longitudinal bars and steel shear connectors with the load applied to the facade wythe; SPS = structural wythe with the ribs on the compression side; SSF = identical to SPF except load applied on the structural wythe; SSS = structural wythe with the ribs on the tension side. 1 mm = 0.0394 in.; 1 kN = 0.225 kip.

side. After connector failure (Fig. 8), there was a decrease in load and stiffness, but the load eventually reached a second peak.

The ultimate load of both specimens BPF and BPS coincided with the onset of concrete crushing in the shear span immediately to the support side of the loading point (Fig. 8). Crushing was gradual, and the load decreased slowly as deflection increased. Both tests were concluded when the actuator reached full stroke (Fig. 8). Relative to peak loads at this point, the loads in specimens BPF and BPS were 84% and 70%, respectively. Specimen BPF had complete failure of all shear connectors on one side (Fig. 8). Specimens BPF and BPS failed to achieve their potential flexural capacity because of the shear-compression failure in the region immediately beyond the constant moment zone.

The reduction in specimen BPS was minor. It achieved 90% of the expected flexural strength. However, specimen BPF was not close to its potential flexural capacity. Relative to steel-reinforced members with equal reinforcement ratios, FRP-reinforced members have lower shear capacity because the lower stiffness of the longitudinal reinforcement increases crack widths and height, which limits aggregate interlock and reduces the compression zone. For specimen BPF, the ultimate strength was 1.65 times that of specimen BPS without a facade, lower than the increases seen when using steel longitudinal reinforcement. This reduction is due to the failure of the shear connection prior to that of the member, which was not observed in the other panels (even specimen HPF, which had BFRP shear connectors).

Similar to specimen HPF, once shear connectors began to fail on one side in specimen BPF, wythe slip on the other side remained almost constant. When specimen BPF was unloaded, the slip on the one end of specimen BPF was 34 mm (1.3 in.), while the other side had 3.4 mm (0.13 in.). The side with higher slip is where concrete crushed. The load-slip behavior of specimens BPF and HPF were similar at low loads but diverged around 35 kN (7.8 kip) as flexural crack propagation progressed in specimen HPF.

With the exception of the crushed region, the crack patterns of the BFRP-reinforced panels were similar to those of the steel-reinforced ones. As indicated previously, cracks in the BFRP-reinforced panels were wider (by about six times at the same load) than their steel-reinforced counterparts.

The strain gauges in specimens BPF and BPS (Fig. 10) behaved as expected until the onset of shear failure. Shear failure caused a decrease in the longitudinal reinforcement strain as forces redistributed. Shear-connector failure in BPF caused a region of decreased strain because deformation occurring elsewhere was not captured by the gauge.

Panels' responses relative to theoretically noncomposite and fully composite panels

The panels were modeled with structural analysis software[29] using the previously presented material properties

SSS during test

SPS during test

HPF after rupture of structural wythe reinforcement

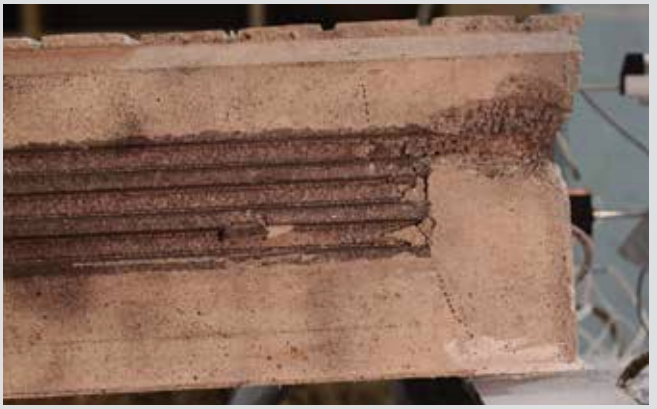

End slip in SPF near failure

Visible slip after failure of BPF

Failed shear connector in BPF

Crushed web in BPS

Excessive deflection observed in BPF prior to unloading

Figure 8. Photos of panels during and after testing. Note: BFRP = basalt-fiber-reinforced polymer; BPF = full panel BFRP-reinforced wall; BPS = structural wythe BFRP-reinforced wall; HPF = same flexural design as SPF but has BFRP shear connectors; SPF = control full-panel reinforced with steel longitudinal bars and steel shear connectors with the load applied to the facade wythe; SPS = structural wythe with the ribs on the compression side; SSS = structural wythe with the ribs on the tension side.

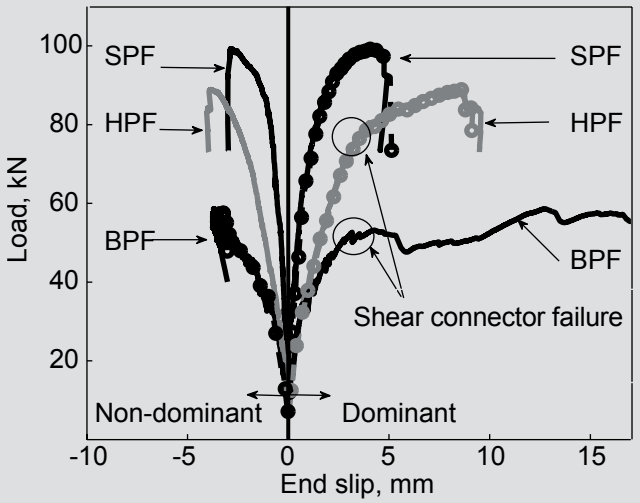

Figure 9. Load-slip responses showing linear potentiometer readings (lines) and digital image correlation results (markers). SSF not shown for clarity but follows the line for SPF until failure. Note: Dominant = end of panel with higher slip and nondominant = end of panel with lower slip. BFRP = basalt-fiber-reinforced polymer; BPF = full panel BFRP-reinforced wall; HPF = same flexural design as SPF but has BFRP shear connectors; SPF = control full-panel reinforced with steel longitudinal bars and steel shear connectors with the load applied to the facade wythe; SSF = identical to SPF except load applied on the structural wythe. 1 mm = 0.0394 in.; 1 kN = 0.225 kip.

to evaluate the fully composite and noncomposite flexural performances of the system. The results (**Table 5**) were compared with those of the test data to evaluate the partial composite action of test specimens. Fully composite panels were modeled as a single cross section made up of both wythes. Noncomposite panels were modeled by running the analysis of the two wythes separately, then summing moments based on the assumption that curvature of both wythes is equal. The theoretical contribution of the facade wythe to moment resistance in the noncomposite system is low relative to that of the structural wythe and accounted for between 9.8% and 17% of the total moment.

The moment-curvature results from the structural analysis software were compared with those calculated from experimental strains measured using the pi gauges in Fig. 8. The panels generally stayed within the two bounds of the structural analysis curves. In specimen SSF, however, the pi gauge did not intercept the crack until near yielding and, as a result, the curvature is underestimated until this point (**Fig. 11**). The moment-curvature responses show that the tested panels have lower stiffness than in the fully composite case and reach higher curvatures at ultimate. The steel-reinforced panels reached ultimate strengths close to those of the fully composite case (Fig. 11). Alternatively, BFRP-reinforced panel specimen BPF had a significantly lower ultimate strength than the fully composite case (Fig. 11) as curvature decreased upon connector failure in specimen BPF, which corresponded to the increase in wythe slip at this point.

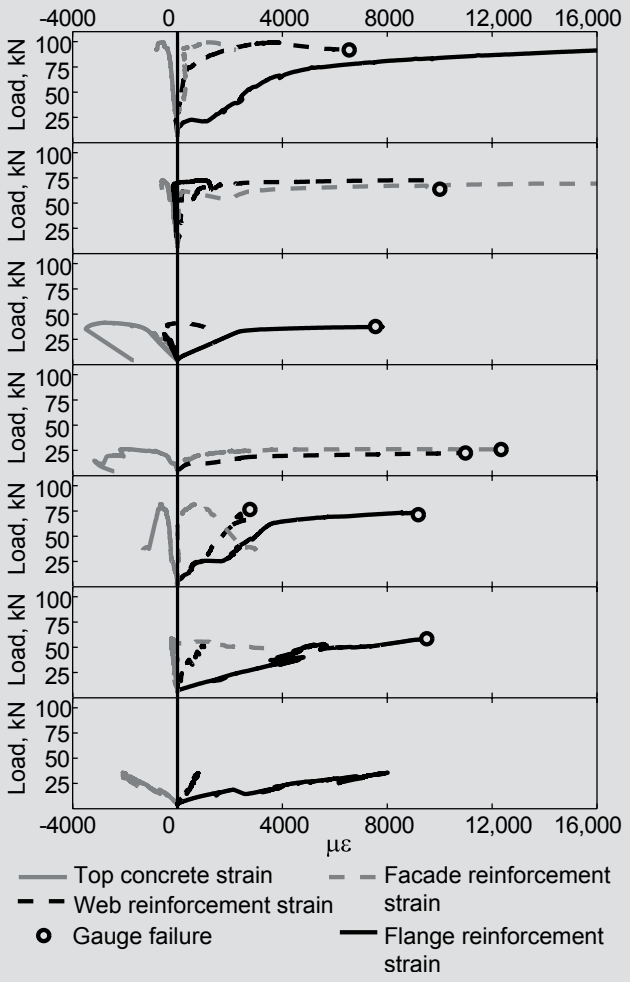

Figure 10. Test load-strain relationships. Note: BFRP = basalt-fiber-reinforced polymer; BPF = full panel BFRP-reinforced wall; BPS = structural wythe BFRP-reinforced wall; HPF = same flexural design as SPF but has BFRP shear connectors; SPF = control full-panel reinforced with steel longitudinal bars and steel shear connectors with the load applied to the facade wythe; SPS = structural wythe with the ribs on the compression side; SSF = identical to SPF except load applied on the structural wythe; SSS = structural wythe with the ribs on the tension side. 1 kN = 0.225 kip.

Rotation and slip from digital image correlation outputs

The slip readings from digital image correlation strongly correlated with those from the linear potentiometers (Fig. 9).

The full digital image correlation output for rotation of the panel ends of specimen SPF at the key test points is also shown on the left side of **Fig. 12**, while the right side of the same figure shows slip distribution through the panel thickness. For rotation, the wythes gave similar readings but rotation values decreased in the foam layer and show that it is deforming rather than slipping due to bond failure at the concrete-foam interface. This is confirmed in the slip readings from digital image correlation, where the accumulation of slip through the foam

Table 5. Ultimate moment comparisons between test and calculated values

Specimen	Test moment resistance, kN-m	Fully composite		Noncomposite	
		Calculated value	Test/calculated	Calculated value	Test/calculated
SPF	51.1	55.6	0.92	19.9	2.57
SSF	37.2	40.2	0.92	15.0	2.48
SPS*	20.9	17.4	1.21	n/a	n/a
SSS*	13.1	12.2	1.07	n/a	n/a
HPF	45.7	55.6	0.82	19.9	2.30
BPF	29.9†	59.4†	0.50†	21.4	1.40
BPS*	17.9†	19.6†	0.91†	n/a	n/a
Facade only: steel	n/a	3.6	n/a	n/a	n/a
Facade ony: BFRP	n/a	4.2	n/a	n/a	n/a

Note: BFRP = basalt-fiber-reinforced polymer; BPF = full panel BFRP-reinforced wall; BPS = structural wythe BFRP-reinforced wall; HPF = same flexural design as SPF but has BFRP shear connectors; n/a = not applicable; SPF = control full-panel reinforced with steel longitudinal bars and steel shear connectors with the load applied to the facade wythe; SPS = structural wythe with the ribs on the compression side; SSF = identical to SPF except load applied on the structural wythe; SSS = structural wythe with the ribs on the tension side. 1 kN-m = 0.737 kip-ft.
*In panels with the structural wythe only, comparison was made with a structural analysis model of the structural wythe only.
†Failure of BPF and BPS was by shear compression, which was not predicted by structural analysis.

layer shows that it is resisting slip rather than failing at the interface. The header's contribution to resisting slip is also seen as it redirects slip to the remaining 60 mm (2.4 in.) of insulation at the panel ends. Although only specimen SPF is depicted in Fig. 12, other tests gave similar outputs.

Assessment of level of partial composite action

By load The composite action by load κ (κ_u at ultimate, κ_y at yielding, and κ_s at service) was evaluated for each key load point using Eq. (3):

$$\kappa = \frac{P_{exp} - P_{NC}}{P_{FC} - P_{NC}} \times 100 \quad (3)$$

where

P_{exp} = observed test load

P_{FC} = theoretical fully composite load

P_{NC} = theoretically fully noncomposite load.

Table 6 shows the results in terms of the calculated κ at ultimate, yielding, and service. Generally, composite action increased as shear-connection stiffness increased: specimen BPF with BFRP connectors had the lowest composite action with values of 20% at service and 24% at ultimate. This is due to the combination of the shear-connector failure and the shear-compression failure preventing the fully composite flexural capacity from being reached.

Alternatively, specimen SPF with steel connectors was consistently about 90% composite at all loading levels, with fully composite behavior limited by shear-connector yielding. Specimen SSF, which had low amounts of slip and no shear-connector failure, had unrealistic values, above 100%, for composite action at service and yielding. This is attributed to variance between theoretical predictions and experimental values, which is likely from the potential shifting of reinforcement location from design and some variability in wythe thickness. Specimen HPF had composite action of 52% at service and 75% at yield and ultimate, lower than specimen SPF due to the lower stiffness of the BFRP.

By deflection The composite action of the walls based on deflection κ_D can also be evaluated at the maximum service load using Eq. (4):

$$\kappa_D = \frac{D_{exp} - D_{NC}}{D_{FC} - D_{NC}} \times 100 \quad (4)$$

where

D_{FC} = theoretical fully composite service stiffness taken from the structural analysis software (in all cases, this was equal to the uncracked stiffness of 53.6×10^{12} N-mm^2 [18.7×10^6 kip-in.^{2}])

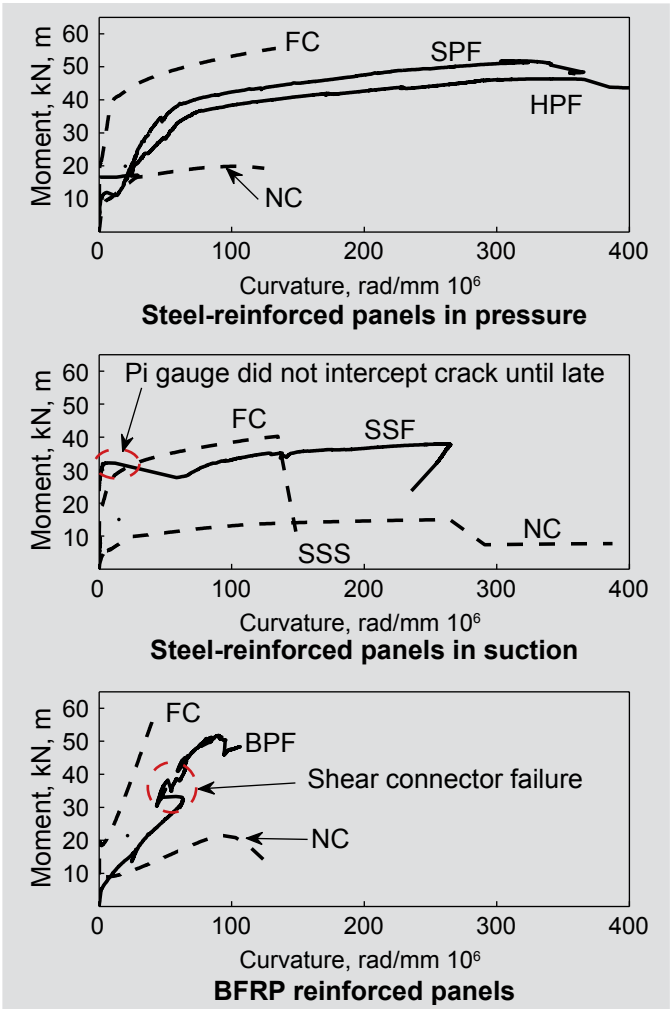

Figure 11. Moment curvature diagrams showing results from tests and the structural analysis software. Note: BFRP = basalt-fiber-reinforced polymer; BPF = full panel BFRP-reinforced wall; FC = full composite; HPF = same flexural design as SPF but has BFRP shear connectors; NC = noncomposite; SPF = control full-panel reinforced with steel longitudinal bars and steel shear connectors with the load applied to the facade wythe; SSF = identical to SPF except load applied on the structural wythe. 1 kN-m = 0.737 kip-in.; 1 rad/mm = 25.4 rad/in.

D_{NC} = noncomposite service stiffness from the structural analysis software

D_{exp} = experimental service stiffness, taken as the average of stiffness estimated using measured midspan deflection D_δ (Eq. [5]) and stiffness estimated using measured end rotation D_ϕ (Eq. [6])

$$D_\delta = \frac{\left(3L^2 - a^2\right)P}{24\delta} \quad (5)$$

$$D_\phi = \frac{a^2\left(L - a\right)L}{2\phi} \quad (6)$$

where

a = shear span length

L = panel span length

δ = midspan deflection

ϕ = end rotation

P = applied load

The stiffness D of a flexural member includes the effects of shear deformation and indirectly incorporates tension stiffening. Both techniques gave similar D results despite being measured from independent techniques. **Table 7** provides a summary of the composite action parameter κ_D at service. The composite action by deflection is lower than that seen by load, with values ranging from 3% and 6.9%. Like the load-based case, κ_D increased with the increase of shear-connection and flexural-reinforcement stiffness.

The κ_D values were quite low, primarily as the high stiffness of the fully composite system (expected to remain uncracked at the maximum service-load value) offset the variations seen across the testing parameters. However, when comparing the stiffness of the tested panels with their theoretically noncomposite values, stiffness decreased 35% when the shear connectors were changed from steel to BFRP (from specimen SPF to HPF) and decreased a further 14% when the longitudinal reinforcement material was changed from steel to BFRP (from specimen HPF to BPF).

Effect of shear-transfer-system stiffness on loads achieved

The shear-transfer system is composed of shear transfer through the foam core, which was well bonded to the concrete and able to absorb shear deformations, and the connector system. The total shear-connection stiffness G_c was established in Eq. (1). This section evaluates the effect of G_c on the yielding and ultimate loads. The highest G_c in this study was that of walls with steel connectors and was 47,200 kN (6120 kip) (Table 1).

The walls with BFRP connectors had a G_c of 25,200 kN (5670 kip) (Table 1). **Figure 13** shows the variation of ultimate and yield loads with G_c for the cases of pressure and suction. For each curve, a third point of G_c equal to 0 (representing a totally noncomposite system) was added to provide a complete trend. This point was established by adding the load (ultimate or yield) from the tested structural (single) wythe to the load (ultimate, yield, or service) of the facade wythe, predicted using the structural analysis software (because the facade was never tested by itself). Figure 13 also shows the ceiling loads (horizontal lines), representing the maximum predicted values based on the assumption of a full composite action. The contribution of foam core only to G_c (second term of Eq. [1]) is also shown as the vertical dotted lines. Figure 13 clearly shows the expected trends that the ultimate and yield

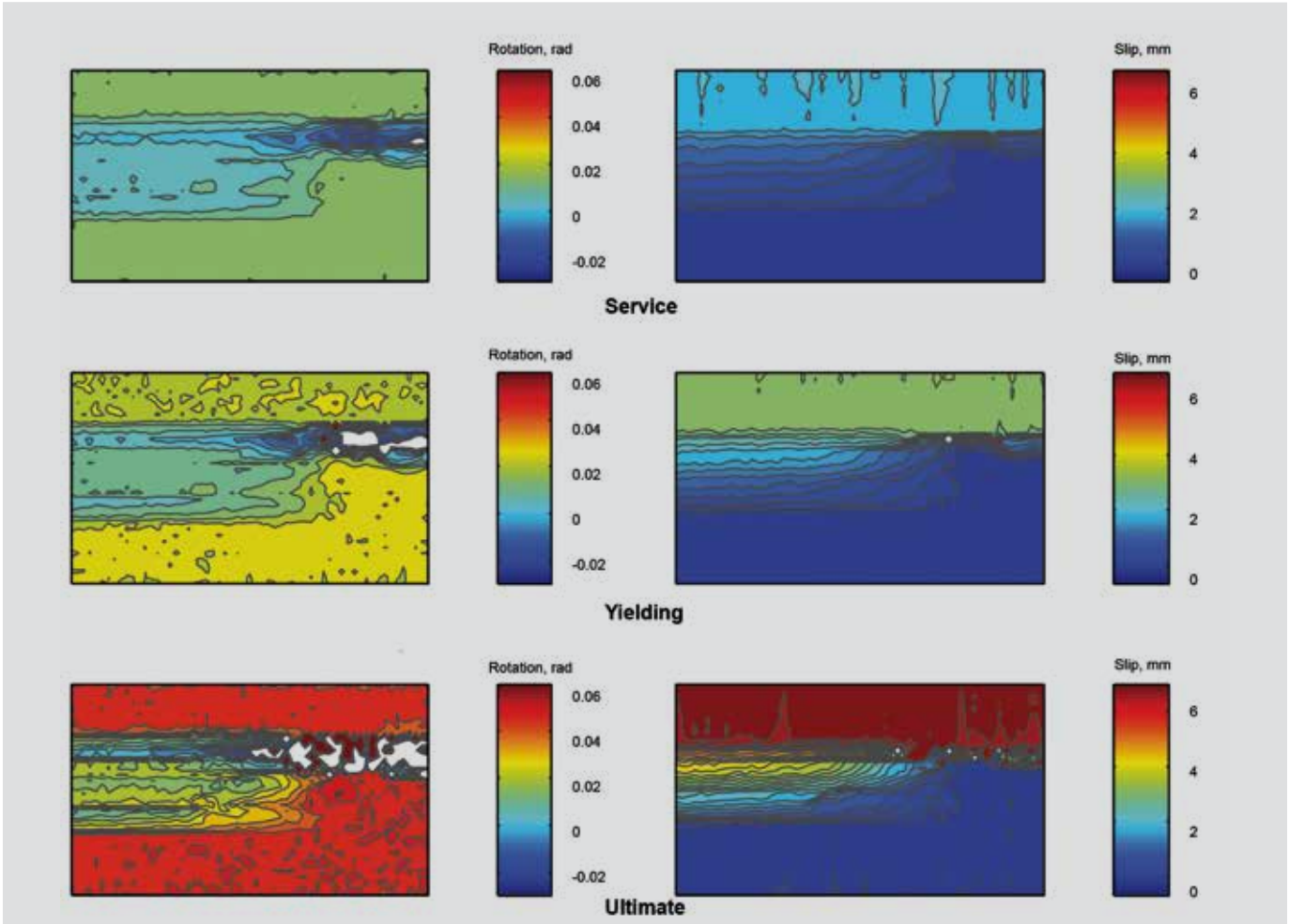

Figure 12. Output of digital image correlation showing values at various load stages in SPF. Note: Left side shows rotation of wythes while right side shows slip relative to the structural (bottom) wythe. The header is seen on the bottom right. Results are similar in other tests. SPF = control full-panel reinforced with steel longitudinal bars and steel shear connectors with the load applied to the facade wythe. 1 mm = 0.0394 in.

loads increase as the overall stiffness G_c of the shear-transfer system increases. The fully composite ultimate and yield loads were approximately double the fully noncomposite loads. The panels with steel connectors approached closely the values of a fully composite system, while the panels with BFRP connectors achieved about 90% of the loads of the panels with steel connectors.

Contribution from the foam core can be conservatively neglected in cases where a designer is concerned that the

Table 6. Composite action by strength methods at key load points

Specimen	Ultimate load, kN			Yield load, kN			Service load, kN			Composite action, %		
	Test value	Fully composite	Fully noncomposite	Test value	Fully composite	Fully noncomposite	Test value	Fully composite	Fully noncomposite	κ_u	κ_y	κ_s
SPF	99.32	107.0	38.20	74.59	77.63	31.71	50.94	54.13	23.52	89	93	90
SSF	72.67	77.37	28.87	58.48	54.50	18.80	50.83	38.71	13.94	91	111	149
HPF	88.90	107.0	38.20	66.25	77.63	31.71	39.36	54.13	23.52	74	75	52
BPF	58.64	114.7	41.22	n/a	n/a	n/a	29.50	56.77	22.85	24	n/a	20

Note: BFRP = basalt-fiber-reinforced polymer; BPF = full panel BFRP-reinforced wall; HPF = same flexural design as SPF but has BFRP shear connectors; n/a = not applicable; SPF = control full-panel reinforced with steel longitudinal bars and steel shear connectors with the load applied to the facade wythe; SSF = identical to SPF except load applied on the structural wythe; κ_s = degree of composite action based on service load; κ_u = degree of composite action based on ultimate load; κ_y = degree of composite action based on yield load. 1 kN = 0.225 kip.

Table 7. Composite action by stiffness methods at service load.

Specimen	Specimen D, $\times 10^{12}$ N-mm^2			Structural analysis D, $\times 10^{12}$ N-mm^2		Composite action κ_D, %
	By deflection	By rotation	Average	Fully composite	Noncomposite	
SPF	5.08	5.13	5.11	53.6	1.77	6.4
SSF	5.52	5.16	5.34	53.6	1.75	3.9
SPS	1.48	1.42	1.45	n/a	n/a	n/a
SSS	1.46	1.31	1.39	n/a	n/a	n/a
HPF	3.81	3.75	3.78	53.6	1.77	6.9
BPF	3.45	3.19	3.32	53.6	1.74	3.0
BPS	1.51	1.52	1.52	n/a	n/a	n/a

Note: BFRP = basalt-fiber-reinforced polymer; BPF = full panel BFRP-reinforced wall; BPS = structural wythe BFRP-reinforced wall; D = panel stiffness; HPF = same flexural design as SPF but has BFRP shear connectors; n/a = not applicable; SPF = control full-panel reinforced with steel longitudinal bars and steel shear connectors with the load applied to the facade wythe; SPS = structural wythe with the ribs on the compression side; SSF = identical to SPF except load applied on the structural wythe; SSS = structural wythe with the ribs on the tension side. 1×10^6 N-mm^2 = 0.345 kip-in.^{2}

foam-concrete bond could fail from freezing and thawing, thermal, or loading cycles. The load corresponding to foam shear only ΔP_{foam} can be estimated by deducting the load at zero shear stiffness from the load corresponding to foam shear only (that is, the load at the vertical dotted line). The loss of foam shear transfer may then be accounted for by deducting ΔP_{foam} from the loads achieved at subsequent shear-stiffness values.

Ductility and deformability

Table 3 presents ductility (for steel-reinforced panels) and deformability (for all panels) factors. The deformability of the full panels was higher than that of their structural counterparts' wythes only. Specimens SPF and SSF had 50% higher J-factors (Eq. [2]) than specimens SPS and SSS. Specimen HPF showed the greatest deformability, which can be linked to the higher amounts of shear deformation in the core region relative to the other panels. Specimen BPF was only slightly higher in deformability than specimen BPS, likely due to the fact that the panel failed by loss of shear connection, which reduced the J-factor moment component. Energy methods consistently gave higher (8% to 22%) estimates of deformability than the J-factor, with the value tending to increase with ultimate load. In flexural members, it is desirable to achieve J-factors equal to or higher than 4.0 because this allows for warning of failure through large excessive deflection and energy dissipation. Aside from specimens SSS and SPS, this held true, but even specimens SSS and SPS had ductility indices greater than 2.0 and provided warning of failure through excessive crack widths at the point of failure.

For steel-reinforced panels, ductility ranged from 2.16 to 3.20 and gave visual warnings of failure through excessive crack widths, particularly at the rupture point. Ductility, highest in specimens HPF and SPF, was increased by the deformation of the shear connectors.

Specimen HPF dissipated the greatest amount of energy through the high degree of shear-connector deformation and yielding of the longitudinal reinforcement. For similar reasons, this was followed by specimen SPF. Specimen BPF, which had excessive deflection at failure and substantial wythe slip, was third. Energy dissipation was higher at all points in the full panels relative to those with the structural wythe alone, and this showed the facade's contribution.

Results compared with design code requirements

The maximum service and factored wind pressures from the *National Building Code of Canada* are 2.07 and 2.9 kPa (0.3 and 0.4 psi), respectively. Based on the loading configuration used in this study, and to achieve the same moments, these values translate into equivalent loads of 4.80 kN (1.08 kip) in service and 6.72 kN (1.52 kip) when factored. Each of the tested panels exceeded these load requirements by factors ranging from 3.5 to 10.6 in service and 3.9 to 14.8 at ultimate.

Conclusion

A precast concrete sandwich panel system was tested in flexure to investigate the impact of flexural-reinforcement material, shear connector material, and panel orientation with respect to loading direction on response, composite action, and failure modes. The results were compared with theoretical fully composite and fully noncomposite values. The following was concluded:

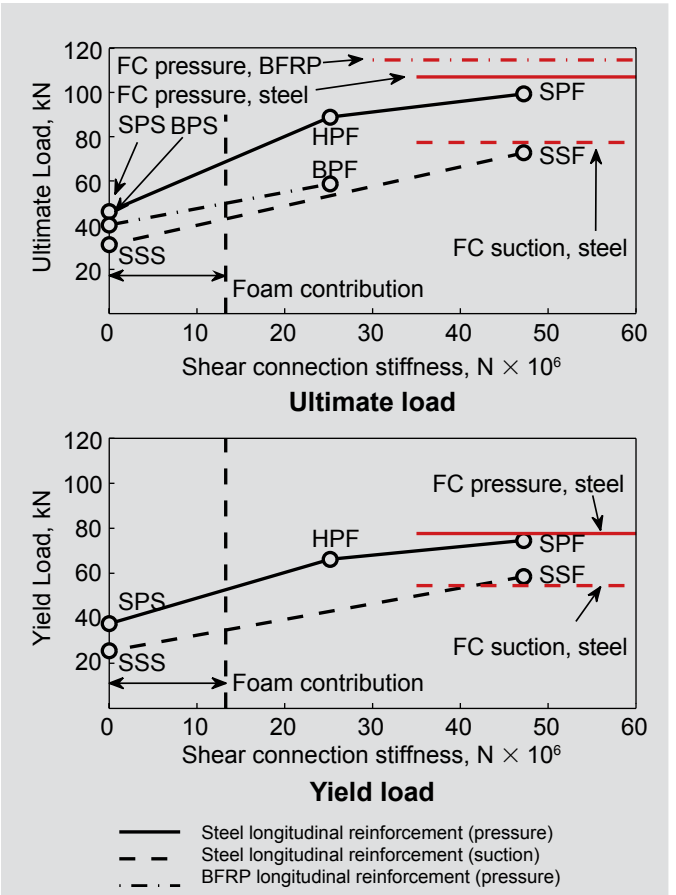

Figure 13. Parameter impact. Note: BFRP = basalt-fiber-reinforced polymer; BPF = full panel BFRP-reinforced wall; FC = full composite; HPF = same flexural design as SPF but has BFRP shear connectors; SPF = control full-panel reinforced with steel longitudinal bars and steel shear connectors with the load applied to the facade wythe; SSF = identical to SPF except load applied on the structural wythe. Note: 1 kN = 0.225 kip.

- Strength-based methods for composite action gave values from 51% to 90% composite action, while stiffness-based techniques gave from 3% to 6.9% composite action. Strength methods should be used for ultimate limit state checks, while stiffness methods should be used for serviceability-limit-state checks. Both methods saw increases in composite action with increases in shear-connection and longitudinal-reinforcement stiffness.

- In steel-reinforced wythes, partial composite action increased the ultimate load of the structural wythe 2.49 times in pressure loading, 2.99 times in simulated suction when steel connectors were used, and 2.21 times in pressure when BFRP ties were used. In BFRP-reinforced wythes with BFRP connectors, partial composite action increased the ultimate load of the structural wythe 1.65 times in pressure loading. This highlights that designing walls using the capacity of a single wythe only may severely underestimate their strength and stiffness.

- The panel with steel-reinforced wythes and BFRP connectors achieved 90% of the flexural strength of the panel with steel-reinforced wythes and steel connectors. In both cases the steel reinforcement ruptured in tension.

- With equal longitudinal reinforcement ratios, rib crushing is more likely to occur with BFRP than with steel reinforcement because the lower reinforcement causes wider cracks, limiting concrete aggregate interlock and reducing the shear capacity. In addition, the higher strength of the reinforcement makes it more likely to cause concrete crushing. This failure mode should be considered in design because designing purely for flexure with BFRP-reinforced walls may overestimate their capacity.

- While BFRP connectors provided less composite action than steel connectors in similar panels with steel-reinforced wythes, the added deformations and deflections at ultimate led to higher deformability factors.

- The BFRP-reinforced panels showed a distinct load plateau after the onset of connector failure, which gave warnings of failure beyond the excessive deflections typically used to provide warnings of failure in FRP-reinforced sections.

- Digital image correlation results can be used to show that the insulation contributes to shear resistance and can detect failure of the insulation-concrete bond. This is not definitively observed using conventional slip-measurement techniques.

In this study the reversed bending induced by wind suction was simulated by flipping the specimen and applying pressure to the structural wythe. Although this technique provides the correct tension and compression in the respective wythes, it does not account for the transverse pulling effect of wind suction, which puts the foam-concrete interface in tension and could weaken the composite action.

In this study, BFRP performed adequately as a shear connector and as longitudinal reinforcement. If considering this material in practice, designers should pay special attention to the lower material stiffness relative to steel with particular focus on the impact on deflections, partial composite action, and shear resistance. The authors recommend that additional research focusing on the long-term performance of BFRP-reinforced sandwich panels subject to fatigue, environmental effects, and axial loading be performed before this material is used in practice.

References

1. Cuddihy, J., C. Kennedy, and P. Byer. 2005. "Energy Use in Canada: Environmental Impacts and Opportunities in Relationship to Infrastructure Systems." *Canadian Journal of Civil Engineering* 32 (1): 1–15.

2. Al-Homoud, M. S. 2005. "Performance Characteristics and Practical Applications of Common Building Thermal Insulation Materials." *Building and Environment* 40 (3): 353–366.

3. Gajda, J. 2001. *Energy Use of Single-Family Houses with Various Exterior Walls*. Skokie, IL: Portland Cement Association.

4. Brown, W. C., P. Eng, D. L. Scott, and D. G. J. Dechamplain. 2001. "Building Science Details for Architectural Precast Concrete Sandwich Panels." In *Thermal Performance of the Exterior Envelopes of Buildings VIII*, 1–13. Atlanta, GA: American Society of Heating, Refrigerating, and Air Conditioning Engineers (ASHRAE). CD-ROM.

5. PCI Committee on Precast Concrete Sandwich Panels. 2011. "State of the Art of Precast/Prestressed Concrete Sandwich Wall Panels." *PCI Journal* 56 (2): 131–176.

6. PCI Committee on Precast Concrete Sandwich Panels. 1997. "State-of-the-Art of Precast/Prestressed Sandwich Wall Panels." *PCI Journal* 42 (2): 1–61.

7. Maximos, H. N., W. A. Pong, M. K. Tadros, and L. D. Martin. 2007. *Behavior and Design of Composite Precast Prestressed Concrete Sandwich Panels with NU-Tie*. Lincoln, NE: University of Nebraska–Lincoln.

8. Benayoune, A., A. A. A. Samad, D. N. Trikha, A. A. Abang Ali, and S. H. M. Ellinna. 2008. "Flexural Behaviour of Pre-cast Concrete Sandwich Composite Panel — Experimental and Theoretical Investigations." *Construction and Building Materials* 22 (4): 580–592.

9. Hassan, T. K., and S. H. Rizkalla. 2010. "Analysis and Design Guidelines of Precast, Prestressed Concrete, Sandwich Wall Panels Reinforced with CFRP Grid." *PCI Journal* 55 (2): 147–162.

10. Lee, B. J., and S. Pessiki. 2008. "Revised Zone Method *R*-Value Calculation for Precast Concrete Sandwich Panels Containing Metal Wythe Connectors." *PCI Journal*, 53 (5): 86–100.

11. Allen, H. G. 1969. *Analysis and Design of Structural Sandwich Panels*. Oxford, England: Pergamon Press.

12. McCall, W. 1985. "Thermal Properties of Sandwich Panels." *Concrete International* 7 (1): 35–41.

13. Frankl, B. A., G. W. Lucier, and T. K. Hassan. 2011. "Behavior of Precast, Prestressed Concrete Sandwich Wall Panels Reinforced with CFRP Shear Grid." *PCI Journal* 56 (1): 42–54.

14. Pessiki, S., and A. Mlynarczyk. 2003. "Experimental Evaluation of the Composite Behavior of Precast Concrete Sandwich Wall Panels." *PCI Journal* 48 (2): 54–71.

15. Woltman, G., D. Tomlinson, and A. Fam. 2013. "Investigation of Various GFRP Shear Connectors for Insulated Precast Concrete Sandwich Wall Panels." *Journal of Composites for Construction* 17 (5): 711–721.

16. Tomlinson, D., and A. Fam. 2014. "Experimental Investigation of Precast Concrete Insulated Sandwich Panels with Glass Fiber-Reinforced Polymer Shear Connectors." *ACI Structural Journal* 111 (3): 595–606.

17. Brik, V. 2003. *Advanced Concept Concrete Using Basalt Fiber/BF Composite Rebar Reinforcement*. Washington: DC: Transportation Research Board.

18. Naito, C., J. Hoemann, M. Beacraft, and B. Bewick. 2012. "Performance and Characterization of Shear Ties for Use in Insulated Precast Concrete Sandwich Wall Panels." *Journal of Structural Engineering* 138 (1): 52–61.

19. Tomlinson, D. G., N. Teixeira, and A. Fam. 2014. "Comparison of Steel and Basalt-FRP Angled Shear Connectors in Precast Concrete Sandwich Wall Panels" In *60th PCI Convention and National Bridge Conference*. Chicago, IL: PCI.

20. Wu, G., X. Wang, Z. Wu, Z. Dong, and G. Zhang. 2015. "Durability of Basalt Fibers and Composites in Corrosive Environments." *Journal of Composite Materials* 49 (7): 873–887.

21. Sim, J., C. Park, and D. Y. Moon. 2005. "Characteristics of Basalt Fiber as a Strengthening Material for Concrete Structures." *Composites Part B: Engineering* 36 (6–7): 504–512.

22. ASHRAE. 2010. *Energy Standard for Buildings except Low-Rise Residential Buildings*. ASHRAE 90.1. Atlanta, GA: ASHRAE.

23. CSA (Canadian Standards Association). 2004. *Design of Concrete Structures*. CAN/CSA-A23.3-04. Rexdale, ON, Canada: CSA.

24. ACI (American Concrete Institute) Committee 318. 2014. *Building Code Requirements for Structural Concrete (ACI 318-14) and Commentary (ACI 318R-14)*. Farmington Hills, MI: ACI.

25. Take, W. A., M. D. Bolton, and D. J. White. 2003. "Soil Deformation Measurement Using Particle Image

Velocimetry (PIV) and Photogrammetry." *Géotechnique* 53 (7): 619–631.

26. National Research Council of Canada. 2005. *National Building Code of Canada*. NBCC-2005. Ottawa, ON, Canada: National Research Council of Canada.

27. Newhook, J., A. Ghali, and G. Tadros. 2002. "Concrete Flexural Members Reinforced with Fiber Reinforced Polymers: Design for Cracking and Deformability." *Canadian Journal of Civil Engineering* 29 (1): 125–134.

28. Theriault, M., and B. Benmokrane. 1998. "Effects of FRP Reinforcement Ratio and Concrete Strength on Flexural Behaviour of Concrete Beams." *Journal of Composites for Construction* 2 (1): 7–16.

29. Bentz, E. C. 2000. "Sectional Analysis of Reinforced Concrete Members." PhD thesis, University of Toronto, Toronto, ON, Canada.

Notation

a = shear span length

A = gross reinforcement cross-sectional area

A_g = gross concrete cross-sectional area

A_{in} = insulation foam area subject to shear

A_{sc} = shear connector cross-sectional area

D = stiffness

D_{exp} = experimental service stiffness incorporating shear deformation through the insulation layer

D_{FC} = theoretical fully composite service stiffness

D_{NC} = theoretical noncomposite service stiffness

D_{δ} = experimental service stiffness incorporating shear deformation evaluated based on deflections

D_{ϕ} = experimental service stiffness incorporating shear deformation evaluated based on end rotation

DL = dead load

E = reinforcement modulus of elasticity

E_{sc} = shear connector modulus of elasticity

f_y = steel yield stress

G_c = effective shear-connection stiffness accounting for both connector and insulation contribution

G_{in} = shear modulus of insulation foam

L = panel span length

LL = live load

M_u = midspan moment at ultimate

M_{NL} = midspan moment at point of first material nonlinearity

n = number of shear connectors

P = applied load

P_{exp} = observed experimental load

P_{FC} = theoretically fully composite section load

P_{NC} = theoretically noncomposite section load

UL = ultimate load

ΔP_{foam} = load corresponding to foam shear only

Δ_u = midspan deflection at ultimate

Δ_y = midspan deflection at yielding

δ = midspan deflection

δ_{NL} = midspan deflection at point of first material nonlinearity

δ_u = midspan deflection at ultimate

ε_c = concrete strain

θ = shear connector insertion angle

κ = degree of composite action

κ_D = degree of composite action based on member stiffness

κ_s = degree of composite action based on service load

κ_u = degree of composite action based on ultimate load

κ_y = degree of composite action based on yield load

Φ = member deformability

ϕ = wythe end rotation

About the authors

Douglas G. Tomlinson is a PhD candidate and Canada Foundation for Innovation project manager in the Department of Civil Engineering at Queen's University in Kingston, ON, Canada.

Amir Z. Fam, PhD, PEng, is a professor and the Donald and Sarah Munro Chair in Engineering and Applied Science for the Department of Civil Engineering at Queen's University.

Abstract

A single-story precast concrete insulated sandwich wall panel design was tested in flexure. Testing parameters included shear-connector and flexural-reinforcement material type, namely steel and basalt-fiber-reinforced polymer (BFRP). BFRP connectors have the advantage of lower thermal bridging than conventional metallic connectors. Some walls were tested without facade wythes to quantify the additional capacity contributed by the facade through partial composite action. Steel-reinforced walls showed a strength-based composite action exceeding 90% with steel connectors and 75% with BFRP connectors. Alternatively, BFRP-reinforced walls with BFRP connectors showed only 51% composite action. When evaluating composite action by deflection, rather than load, the walls had substantially lower values, ranging from 3% to 6.9%. BFRP-reinforced panels had lower strength than the steel-reinforced panels because they were prone to shear-compression failure but had higher deflections at ultimate. Shear deformation between wythes increased deformability, with the highest value observed in a panel with BFRP connectors and steel flexural reinforcement. Digital image correlation was used to determine wythes' relative slip and rotations at the panel ends. The wall design performed adequately as a non-load-bearing wall based on building-code requirements for maximum wind pressure.

Keywords

Basalt, facade, fiber-reinforced polymer, FRP, partially composite, sandwich panel, shear connector, structural wythe.

Review policy

This paper was reviewed in accordance with the Precast/Prestressed Concrete Institute's peer-review process.

Reader comments

Please address reader comments to journal@pci.org or Precast/Prestressed Concrete Institute, c/o *PCI Journal*, 200 W. Adams St., Suite 2100, Chicago, IL 60606.